Available online at www.sciencedirect.com
ScienceDirect
Journal of Molecular Graphics and Modelling 26 (2008) 1125–1130
Journal of Molecular Graphics and Modelling
www.elsevier.com/locate/JMGM

Computation of through-space NMR shielding effects in aromatic ring π-stacked complexes

Ned H. Martin [a,*], Ruth M. Floyd [a], H. Lee Woodcock [a,1], Scott Huffman [a,2], Chang-Kiu Lee [b]

[a] *Department of Chemistry and Biochemistry, University of North Carolina Wilmington, 601 S. College Road, Wilmington, NC 28403-5932, USA*
[b] *Department of Chemistry, Kangwon National University, Chuncheon, 200-701, South Korea*

Received 10 July 2007; accepted 3 October 2007
Available online 9 October 2007

Abstract

Aromatic compounds can form dimeric complexes in solution. Substituted aromatics tend to form parallel-stacked complexes, either aligned or offset. The HF-GIAO method in Gaussian 03 was employed to calculate the NMR isotropic shielding values of the proximal hydrogen of diatomic hydrogen probes above and below the center of the ring and above and below an unsubstituted ring carbon of 1,3,5-trimethylbenzene in a face-to-face π-stacked aligned complex with 1,3,5-trinitrobenzene. The calculated isotropic shielding values for the aromatic hydrogens of each of the substituted rings were subtracted from the isotropic shielding values calculated for the comparable positions in the complex. Complexation results in each aromatic ring shielding the other ring. Also, the calculated isotropic shielding values for the proximal hydrogen of a diatomic hydrogen probe over (or under) each of the individual substituted benzenes were subtracted from the isotropic shielding values calculated for the comparable positions in the complex. The difference is the shielding increment due to complexation. Complexation results in increased NMR shielding of a hydrogen probe molecule on both sides of the π-stacked complex, with slightly more shielding due to complexation on the side nearest 1,3,5-trimethylbenzene. The results are interpreted in terms of polarization of the π cloud of the substituted benzenes by complexation and its NMR consequences. Finally, NMR shielding calculations were done on the optimized structure of *N*-phenylpyrrole dimer. The data were compared to concentration-dependent NMR shift data to estimate the percent dimer present.
© 2007 Elsevier Inc. All rights reserved.

Keywords: NMR; Through-space shielding effects; HF-GIAO calculations; Aryl–aryl π-stacked complex; Concentration-dependent NMR chemical shifts

1. Introduction

The results of HF-GIAO [1] calculations to determine through-space NMR shielding effects, to map the resulting through-space NMR shielding increments, and to develop through-space NMR shielding equations for a number of common organic functional groups, including the benzene ring [2,3], the carbon–carbon double bond [4–7], the carbon–carbon triple bond, the carbon–nitrogen triple bond, the nitro group [8], the carbonyl group [9], and functional groups common to peptides [10] have been reported. Recently the NMR shielding surfaces of some simple aromatic and antiaromatic hydrocarbons were described [11]. The synergistic effect on NMR shielding of complexation of cations with aromatic rings has also been reported [12]. The shielding predictions derived from calculations of small molecule models of various functional groups have proven to be successful at accurately predicting through-space chemical shift effects in more complex molecules that contain those functional groups. We now report results of a computational study of the through-space NMR shielding of a diatomic hydrogen probe molecule by aromatic ring-aromatic ring π complexes. Knowledge of these through-space shielding effects should aid in understanding the NMR spectra and in determining the structure of molecules that

* Corresponding author. Tel.: +1 910 962 3453; fax: +1 910 962 3013.
E-mail address: martinn@uncw.edu (N.H. Martin).
[1] Present address: Laboratory of Computational Biology, National Heart Lung and Blood Institute, National Institutes of Health, Bethesda, MD 20892, USA.
[2] Present address: Department of Chemistry and Physics, Western Carolina University, Cullowhee, NC 29723, USA.

1093-3263/$ – see front matter © 2007 Elsevier Inc. All rights reserved.
doi:10.1016/j.jmgm.2007.10.004

possess these features, and may help in understanding concentration-dependent NMR spectra.

2. Computational methods

Models of π-stacked dimeric complexes of 1,3,5-trimethylbenzene (mesitylene) and 1,3,5-trinitrobenzene of various starting geometries were built in Titan [13] and geometry optimized at the Hartree-Fock level of theory using a 6-31G(d,p) basis set [14]. The lowest energy complex had one aromatic ring parallel to and directly over the other ring, with their substituted carbons aligned (''aligned'', Fig. 1). This was slightly lower in energy than the complex having one aromatic ring parallel to and directly over the other, but rotated 60° (''*ortho*'', Fig. 1). Parallel offset geometries and T-shaped complexes were higher in energy (structures and data not shown). Sinnokrot and Sherrill have reported similar results in their high accuracy quantum mechanical studies of substituted benzene dimers [15,16]. The equilibrium distance between the planes of the substituted aromatic rings was 4.0 Å (Fig. 2). Two diatomic hydrogen (H_2) probes [17] previously geometry optimized at HF/6-31G(d,p) were placed along the axis perpendicular to the center of the aromatic rings with the proximal hydrogen of each at a distance of 2.5 Å from the plane of the ring carbons of the closest ring. (Fig. 3a). A single point NMR calculation was performed on this supramolecule using Gaussian 03 [18] running on an IBM P690 Power 4 using the same method and basis set. This process was repeated with the H_2 probes at proximal hydrogen distances of 3.0, 3.5, 4.0 and 4.5 Å from the plane of the ring carbon atoms. Another set of

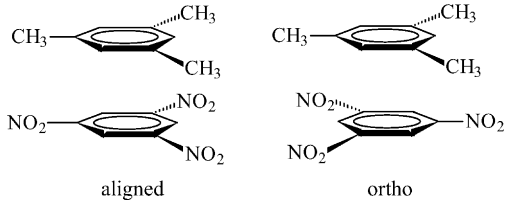

Fig. 1. Orientation of the lowest energy complex (aligned) and the second energy complex (*ortho*).

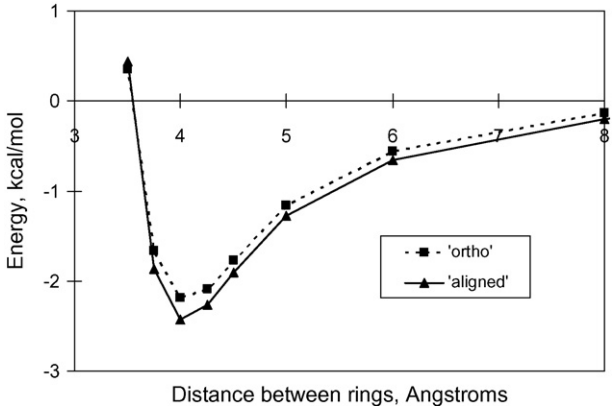

Fig. 2. Graph of HF energy *vs.* distance between the planes of 1,3,5-trimethylbenzene and 1,3,5-trinitrobenzene in the two lowest energy complex geometries.

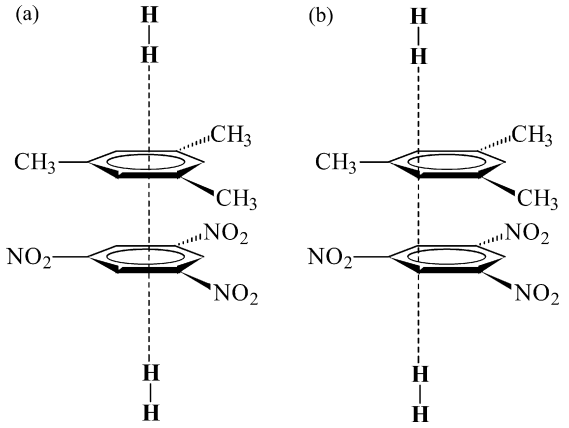

Fig. 3. Structure of complex with (a) diatomic hydrogen probes over the ring center and (b) diatomic hydrogen probes over an unsubstituted ring carbon.

calculations was performed having both of the H_2 probes oriented perpendicular to the rings at a position 2.5 Å from the plane of the ring carbons and having *X* and *Y* coordinates matching those of an unsubstituted ring carbon (Fig. 3b). Single point NMR calculations were performed with the H_2 probes at proximal hydrogen distances of 2.5, 3.0, 3.5, 4.0 and 4.5 Å from the plane of the ring carbon atoms. The modest size 6-31G(d,p) basis set and the HF level of theory (which neglects electron correlation effects) were selected because previous work has shown that this combination gives good results in predicting relative chemical shift effects [2–12]. Inclusion of electron correlation by using MP2 calculations coupled with the 6-31G(d,p) basis set gave comparable results but at a considerably increased computational cost. The more modest basis set and HF theory were selected for their economy and utility in this application. The counterpoise method of Boys and Bernardi [19] was employed to estimate the basis set superposition error (BSSE). All shielding values reported are corrected for BSSE.

The shielding increment ($\Delta\sigma$) at a given point in Cartesian space was determined by subtracting the calculated isotropic shielding value of one of the hydrogens in H_2 (by itself) from the isotropic shielding value of the proximal hydrogen of the H_2 probe in the aryl–aryl π complex. The shielding increments ($\Delta\sigma$) are therefore equal in magnitude but opposite in sign to differences in ^{1}H NMR chemical shifts ($\Delta\delta$).

Because of its greater computational economy, density functional theory (DFT) energy calculations were used to compute the potential energy surface of dimers of previously geometry-optimized *N*-phenylpyrrole. The generalized gradient approximation (gga) exchange functional [20] was employed with a double numerical with polarization (dnp) basis set in DMol3 [21]. Multiple single point calculations were performed on parallel π-stacked geometries of a dimer having the rings aligned antiparallel in which one monomer was moved in the *X* or *Y* direction relative to the other in sequential calculations (Fig. 4). The lowest energy structure was submitted for a geometry optimization to attain the equilibrium conformation and energy. NMR calculations were then performed on this geometry using the GIAO-HF/6-31G(d,p) method.

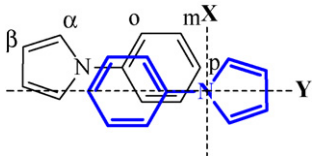

Fig. 4. Cartoon representation of the relative orientation of *N*-phenylpyrrole monomers in the potential energy search for the equilibrium structure of the π complex dimer.

3. Results and discussion

The GIAO-computed isotropic shielding value (26.77 ppm) of a proton in diatomic hydrogen (by itself) was subtracted from those computed for the proximal proton of the diatomic hydrogen probe in some position relative to either the complex or one of the isolated trisubstitued aromatic rings to provide the shielding increment ($\Delta\sigma$). The proximal hydrogen of the diatomic hydrogen probe was shielded to a greater extent (more positive $\Delta\sigma$) over either ring in the π complex than when it was in a comparable position relative to either trisubstituted aromatic ring individually. The shielding increment data for the proximal proton of a molecular hydrogen probe over the center of an aromatic ring are shown in Table 1. The shielding increment was greater over the trinitro substituted ring than over the trimethyl substituted ring, but the effect due to complexation (i.e., the difference between the $\Delta\sigma$ over the complex and that over the isolated aromatic ring) was greater over the trimethyl substituted ring than over the trinitro substituted ring. The ratio of this difference (over the center of the ring) due to complexation near the trimethyl substituted ring to that at the same position relative to the trinitro substituted ring was quite constant at 1.3.

The shielding increment data for the proximal proton of a molecular hydrogen probe over an unsubstituted carbon of an aromatic ring are shown in Table 2. As was observed for the probe over the center of the ring, the shielding increment for a probe over an unsubstituted carbon of the complex was greater over the trinitro substituted ring than over the trimethyl substituted ring, and likewise the effect due to complexation was greater over the trimethyl substituted ring than over the trinitro substituted ring. The ratio of this difference (over an unsubstituted ring carbon) due to complexation near the trimethyl substituted ring to that at the same position relative to the trinitro substituted ring varied from 1.3 to 1.5.

Differences in the Weinhold natural population analysis (npa) computed charges [22–24], calculated using HF/6-31(d,p) on the proximal hydrogen of the diatomic hydrogen probe molecule over the ring center at various distances over the plane of the carbon atoms of the isolated trisubstituted aromatic rings and their complexes are listed in Table 3. Complexation results in a more negative charge on the proximal hydrogen over the center of the trimethyl substituted ring and a more positive charge on the proximal hydrogen over the center of the trinitro substituted ring. Although the magnitude of polarization of the diatomic hydrogen seems small, our previous calculations have shown that this effect may contribute significantly to shielding (or deshielding), and is ignored by the McConnell model that is sometimes used to predict through-space shielding effects.

Differences in the Weinhold natural population analysis (npa) computed charges on the proximal hydrogen of the diatomic hydrogen probe molecule over an unsubstituted ring carbon at various distances over the plane of the carbon atoms of the isolated trisubstituted aromatic rings and complexes are listed in Table 4. Again, complexation results in a more negative charge on the proximal hydrogen over an unsubstituted carbon of the trimethyl substituted ring and a more positive charge on the proximal hydrogen over an unsubstituted carbon of the trinitro substituted ring. The charge differences for the hydrogen probe over an unsubstituted carbon due to

Table 1
Isotropic shielding increment values (ppm) of the proximal proton of the H_2 probe above the center of the ring at 2.5, 3.0, 3.5, 4.0 and 4.5 Å above the plane of the substituted aromatic ring (alone) or in a π complex, their differences, and ratios of the differences

	Distance (Å) above plane of carbons in ring				
	2.5 Å	3.0 Å	3.5 Å	4.0 Å	4.5 Å
$(CH_3)_3$ substituted ring, complex	2.90	1.84	1.25	0.90	0.67
$(CH_3)_3$ ring alone	2.61	1.61	1.06	0.74	0.53
Difference, complex-ring alone	0.29	0.23	0.19	0.16	0.14
$(NO_2)_3$ substituted ring, complex	3.56	2.35	1.65	1.21	0.92
$(NO_2)_3$ substituted ring alone	3.34	2.17	1.50	1.09	0.81
Difference, complex-ring alone	0.22	0.18	0.15	0.12	0.11
Ratio of differences	1.3	1.3	1.3	1.3	1.3

Table 2
Isotropic shielding increment values (ppm) of the proximal proton of the H_2 probe above an unsubstituted carbon at 2.5, 3.0, 3.5, 4.0 and 4.5 Å above the plane of the substituted aromatic ring (alone) or in a π complex, their differences, and ratios of the differences

	Distance (Å) above plane of carbons in ring				
	2.5 Å	3.0 Å	3.5 Å	4.0 Å	4.5 Å
$(CH_3)_3$ substituted ring, complex	1.10	1.07	0.87	0.68	0.54
$(CH_3)_3$ ring alone	0.84	0.86	0.69	0.53	0.41
Difference, complex-ring alone	0.26	0.21	0.18	0.15	0.13
$(NO_2)_3$ substituted ring, complex	1.71	1.52	1.21	0.95	0.75
$(NO_2)_3$ ring alone	1.51	1.36	1.09	0.84	0.66
Difference, complex-ring alone	0.20	0.16	0.12	0.11	0.09
Ratio of differences	1.3	1.3	1.5	1.4	1.4

Table 3
Differences (complex-isolated ring) between the Weinhold (npa) computed charges (in esu $\times 10^3$) of the proximal proton of the diatomic hydrogen probe over the center of the ring at 2.5, 3.0, 3.5, 4.0 and 4.5 Å above the plane of each substituted aromatic ring in the π complex and the isolated substituted aromatic ring

	Distance (Å) above plane of carbons in ring				
	2.5 Å	3.0 Å	3.5 Å	4.0 Å	4.5 Å
$(CH_3)_3$ substituted	−2.5	−2.2	−1.8	−1.5	−1.3
$(NO_2)_3$ substituted	1.8	1.5	1.2	1.0	0.8

Table 4
Differences (complex-isolated ring) between the Weinhold (npa) computed charges (in esu $\times 10^3$) of the proximal proton of the diatomic hydrogen probe over an unsubstituted ring carbon at 2.5, 3.0, 3.5, 4.0 and 4.5 Å above the plane of each substituted aromatic ring in the π complex and the isolated substituted aromatic ring

	Distance (Å) above plane of carbons in ring				
	2.5 Å	3.0 Å	3.5 Å	4.0 Å	4.5 Å
$(CH_3)_3$ substituted	−2.2	−2.1	−1.8	−1.5	−1.3
$(NO_2)_3$ substituted	1.5	1.3	1.1	0.9	0.7

complexation are generally slightly less than those computed for over the ring center.

The aryl ring protons of each substituted aromatic ring in the π complex are more shielded than their counterparts in the isolated rings (Table 5). The magnitude of the shielding on the aromatic hydrogens is independent of the distance of the probe molecule from the ring, thus ruling out any effect of the probe molecule itself. The protons on the trimethyl substituted ring were somewhat more shielded (0.44 ppm) than those on the trinitro substituted ring (0.33 ppm). Each aromatic ring in the dimeric complex is within the shielding region [2,3] of the other aromatic ring, accounting for the observed shielding effect. The difference in the magnitude of shielding is likely due to polarization of the π electrons which results from complexation, a phenomenon previously observed in aromatic ring-cation complexes [12], in which a synergistic effect on shielding was observed upon complexation.

Lee et al. have reported that *N*-phenypyrole exhibits a concentration-dependent NMR spectrum [25]. This phenomenon is not uncommon in heterocyclic aromatic compounds [26–28]. The effect has usually been attributed to dimerization or other aggregation, possibly due to π complex formation, but without proof. In an effort to model this effect, DFT calculations were done on various orientations of two *N*-phenylpyrrole molecules near one another. The DFT geometry optimized monomer of *N*-phenylpyrrole has a 36° dihedral angle between the phenyl ring and the pyrrole ring. In the lowest energy dimer, the monomers were stacked antiparallel so that the phenyl ring of one was parallel to the pyrrole ring of the other with a separation of 4.0 Å. In a series of single point (energy) calculations, one ring was displaced in 1 Å increments in the *X* and *Y* directions starting with the nitrogen atoms above

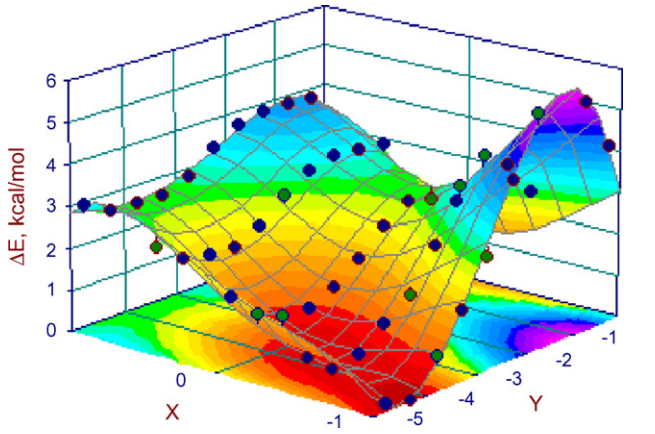

Fig. 5. Graph of DFT energy *vs.* lateral displacement of one molecule of *N*-phenylpyrrole to another in an antiparallel stacked orientation having the phenyl rings 4.0 Å apart.

one another (Fig. 4). The relative energy of each dimer calculated in this way was plotted *vs. X* and *Y* position (Fig. 5). The equilibrium structure of the dimer from the DFT calculation was then optimized using HF/6-31G(d,p), followed by a single point GIAO calculation. A similar series of calculations was performed on tetramethysilane (TMS) and on a monomer of *N*-phenylpyrrole. Subtraction of the mean TMS proton isotropic shielding values from those of the dimeric *N*-phenylpyrrole complex gave estimates of the chemical shifts of each of the protons in the dimer. Mean values of isotropic shieldings were used for each duplicated proton (α, β, o, and m) because it was assumed that the weak aggregate would be in rapid dynamic equilibrium with monomer on the NMR time scale and that this would lead to NMR equivalence of the two α, β, o, and m protons. The difference in the isotropic shielding values of the protons in the optimized *N*-phenylpyrrole monomer and TMS gave estimates of the chemical shifts of the monomer. When the mean chemical shifts of protons in the equilibrium structure dimer are compared to those in the monomer (Table 6), the shielding effect due to complex formation is apparent. Using published data on the chemical shift difference at two concentrations (0.01 and 0.10 M) [25] and assuming a linear relationship between chemical shift change and dimerization, it can be estimated that the 0.1 M solution consisted of at least 13% dimer. It is noteworthy that experimentally only a very slight change in the chemical shift

Table 5
Differences (complex-ring alone) in the isotropic shielding values (ppm) of the aryl protons of each aromatic ring with the diatomic hydrogen probe(s) at 2.5, 3.0, 3.5, 4.0 and 4.5 Å above the center of that substituted aromatic ring (alone) or the π complex

	Distance (Å) above plane of carbons in ring				
	2.5 Å	3.0 Å	3.5 Å	4.0 Å	4.5 Å
Difference above $(CH_3)_3$ substituted ring	0.44	0.44	0.44	0.44	0.44
Difference above $(NO_2)_3$ substituted ring	0.33	0.33	0.33	0.33	0.33

Table 6
Differences in computed chemical shifts (in ppm) of the protons of *N*-phenylpyrrole between the dimer and monomer, differences in observed chemical shifts (in ppm) at 0.01 M and 1.0 M, and their ratio

	Δδ (dimer-monomer)	Δδ (0.01–1.0 M)	Ratio
α	0.23	0.04	0.17
β	0.02	0.02	1.00
ortho	0.55	0.06	0.11
meta	0.43	0.06	0.14
para	0.36	0.05	0.14
Mean ratio*			0.13

* Excluding data for the β protons.

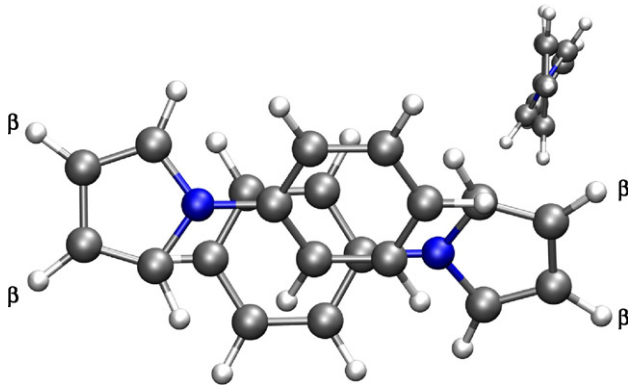

Fig. 6. Equilibrium structure of the π complex dimer of *N*-phenylpyrrole, with side view inset above right.

of the β-protons of phenylpyrrole was observed with changing concentration. The equilibrium structure of the dimer (Fig. 6) shows that the β protons on the pyrrole ring extend well beyond the shielding region of the nearest aromatic ring, and therefore would neither be shielded nor experience a concentration-dependent chemical shift relating to aggregation.

4. Conclusions

The effect of aryl–aryl π complexation between 1,3,5-trimethylbenzene and 1,3,5-trinitrobenzene on the calculated NMR isotropic shielding value of the proximal proton of diatomic hydrogen probes was examined. Each isolated trisubstituted aromatic compound causes shielding of the hydrogen probe; this shielding effect is enhanced over each ring upon complexation. Enhanced polarization of the diatomic hydrogen probes accompanies the shielding due to complexation and is the likely cause of the enhanced shielding effect. The aromatic protons in each ring are also shielded upon forming the dimeric complex. This effect was used to estimate the percent dimer in *N*-phenypyrrole which has concentration dependent NMR chemical shifts.

Acknowledgment

The authors gratefully acknowledge support of this work by the donors of the Petroleum Research Fund, administered by the American Chemical Society.

References

[1] R. Ditchfield, Self-consistent perturbation theory of diamagnetism. I. A gauge-invariant LCAO method for NMR chemical shifts, Mol. Phys. 27 (1974) 553–566.
[2] N.H. Martin, N.W. Allen III, K.D. Moore, L. Vo, A proton NMR shielding model for the face of a benzene ring, J. Mol. Struct. (Theochem.) 454 (1998) 161–166.
[3] N.H. Martin, N.W. Allen III, J.C. Moore, An algorithm for predicting NMR shielding of protons over substituted benzene rings, J. Mol. Graphics Mod. 18 (3) (2000) 242–246.
[4] N.H. Martin, N.W. Allen III, E.K. Minga, S.T. Ingrassia, J.D. Brown, An empirical proton NMR shielding equation for alkenes based on ab initio calculations, Struct. Chem. 9 (6) (1998) 403–410.
[5] N.H. Martin, N.W. Allen III, E.K. Minga, S.T. Ingrassia, J.D. Brown, in: Proceedings of ACS Symposium on Modeling NMR Chemical Shifts: Gaining Insights into Structure and Environment, ACS Press, 1999.
[6] N.H. Martin, N.W. Allen III, E.K. Minga, S.T. Ingrassia, J.D. Brown, An improved model for predicting proton NMR shielding by alkenes based on ab initio GIAO calculations, Struct. Chem. 10 (5) (1999) 375–380.
[7] N.H. Martin, N.W. Allen III, S.T. Ingrassia, J.D. Brown, E.K. Minga, An algorithm for predicting proton deshielding over a carbon–carbon double bond, J. Mol. Graphics Modell. 18 (1) (2000) 1–6.
[8] N.H. Martin, K.H. Nance, Modeling through-space magnetic shielding over the ethynyl, cyano, and nitro groups, J. Mol. Graphics Modell. 21 (2002) 51–56.
[9] N.H. Martin, N.W. Allen III, J.D. Brown, D.M. Kmiec Jr., L. Vo, An NMR shielding model for protons above the plane of a carbonyl group, J. Mol. Graphics Modell. 22 (2003) 127–131.
[10] N.H. Martin, D.M. Loveless, K.L. Main, A.K. Pyles, Computation of through-space shielding effects by functional groups common to peptides, J. Mol. Graphics Modell. 25 (2006) 1–9.
[11] N.H. Martin, D.M. Loveless, K.L. Main, D.C. Wade, Computation of through-space NMR shielding effects by small-ring aromatic and antiaromatic hydrocarbons, J. Mol. Graphics Modell. 25 (2006) 389–395.
[12] N.H. Martin, K.L. Main, A.K. Pyles, Computation of through-space NMR shielding effects by aromatic ring-cation complexes: substantial synergistic effect of complexation, J. Mol. Graphics Modell. 25 (2006) 806–812.
[13] Titan, version 1.0.1, Wavefunction, Inc., Schrödinger, Inc., 1999.
[14] W.J. Hehre, L. Radom, P.v.R. Schleyer, J.A. Pople, Ab Initio Molecular Orbital Theory, Wiley, New York, 1986.
[15] M.O. Sinnokrot, C.D. Sherrill, Substituent effects in π–π interactions: sandwich and T-shaped configurations, J. Am. Chem. Soc. 126 (2004) 7690–7697.
[16] M.O. Sinnokrot, C.D. Sherrill, High-accuracy quantum mechanical studies of π–π interactions in benzene dimers, J. Phys. Chem. A 110 (2006) 10656–10668.
[17] N.H. Martin, D.M. Loveless, D.C. Wade, A comparison of the calculated NMR shielding probes, J. Mol. Graphics Modell. 23 (2004) 285–290.
[18] Gaussian 03, Revision B.01, M.J. Frisch, G.W. Trucks, H.B. Schlegel, G.E. Scuseria, M.A. Robb, J.R. Cheeseman, J.A. Montgomery, Jr., T. Vreven, K.N. Kudin, J.C. Burant, J.M. Millam, S.S. Iyengar, J. Tomasi, V. Barone, B. Mennucci, M. Cossi, G. Scalmani, N. Rega, G.A. Petersson, H. Nakatsuji, M. Hada, M. Ehara, K. Toyota, R. Fukuda, J. Hasegawa, M. Ishida, T. Nakajima, Y. Honda, O. Kitao, H. Nakai, M. Klene, X. Li, J.E. Knox, H.P. Hratchian, J.B. Cross, C. Adamo, J. Jaramillo, R. Gomperts, R.E. Stratmann, O. Yazyev, A.J. Austin, R. Cammi, C. Pomelli, J.W. Ochterski, P.Y. Ayala, K. Morokuma, G.A. Voth, P. Salvador, J.J. Dannenberg, V.G. Zakrzewski, S. Dapprich, A.D. Daniels, M.C. Strain, O. Farkas, D.K. Malick, A.D. Rabuck, K. Raghavachari, J.B. Foresman, J.V. Ortiz, Q. Cui, A.G. Baboul, S. Clifford, J. Cioslowski, B.B. Stefanov, G. Liu, A. Liashenko, P. Piskorz, I. Komaromi, R.L. Martin, D.J. Fox, T. Keith, M.A. Al-Laham, C.Y. Peng, A. Nanayakkara, M. Challacombe, P.M.W. Gill, B. Johnson, W. Chen, M.W. Wong, C. Gonzalez, J.A. Pople, Gaussian, Inc., Pittsburgh PA, 2003.
[19] S.F. Boys, F. Bernardi, The calculations of small molecular interaction by the difference of separate total energies. Some procedures with reduced error, Mol. Phys. 19 (1970) 553–566.
[20] A.D. Becke, Density-functional exchange-energy approximation with correct asymtotic behavior, Phys. Rev. A 38 (1988) 3098–3100.
[21] DMol3, Accelrys, 2005.
[22] A.E. Reed, R.B. Weinstock, F. Weinhold, Natural population analysis, J. Chem. Phys. 83 (1985) 735–746.
[23] A.E. Reed, L.A. Curtiss, F. Weinhold, Intermolecular interactions from a natural bond order, donor–acceptor viewpoint, Chem. Rev. 88 (1988) 899–926.
[24] J.E. Carpenter, F. Weinhold, J. Mol. Struct. (Theochem.) 169 (1988) 41–62.
[25] C.K. Lee, J.H. Jun, J.S. Yu, Synthesis and nuclear magnetic resonance spectroscopic studies of 1-arylpyrroles, J. Hetero. Chem. 37 (2000) 15–24.

[26] A. Mitra, P.J. Seaton, R.A. Assarpour, T. Williamson, Unprecedented concentration dependent chemical shift variation in 1H-NMR studies, Tetrahedron 54 (1998) 15489–15498.
[27] A. Mitra, P.J. Seaton, J.F. Capitani, A. Assarpour, Unprecedented concentration dependent chemical shift variation in ^{1}H-NMR studies: a problem in structure elucidation and the study of molecular recognition, J. Indian Chem. Soc. 75 (1998) 823–830.
[28] P.J. Seaton, R.T. Williamson, A. Mitra, A. Assarpour, Synthesis of quinolines and their characterization by NMR spectroscopy, J. Chem. Educ. 79 (2002) 106–110.